Contents lists available at ScienceDirect

Virus Research

Short communication

Characterization of a putative novel nepovirus from *Aeonium* sp.

Roberto Sorrentino [a], Angelo De Stradis [b], Marcello Russo [b], Daniela Alioto [a],[**],
Luisa Rubino [b],[*]

[a] *Università di Napoli "Federico II", via Università 100, 80055 Portici (NA), Italy*
[b] *Istituto di Virologia Vegetale del CNR, UOS Bari, Via Amendola 165/A, 70126 Bari, Italy*

ABSTRACT

A virus was isolated from potted plants of an unidentified species of *Aeonium*, a succulent ornamental very common in Southern Italy, showing chlorotic spots and rings on both leaf surfaces. It was successfully transmitted by sap inoculation to a limited range of hosts, including *Nicotiana benthamiana* which was used for ultrastructural observations and virus purification. Virus particles are isometric, *ca.* 30 nm in diameter, have a single type of coat protein (CP) subunits 54 kDa in size, that encapsidate single-stranded positive-sense RNA species of 7549 (RNA1) and 4010 (RNA2) nucleotides. A third RNA molecule 3472 nts in size entirely derived from RNA2 was also found. The structural organization of both genomic RNAs and the cytopathological features were comparable to those of nepoviruses. In addition, amino acid sequence comparisons of CP and the Pro-Pol region (a sequence containing parts of the proteinase and polymerase) with those of other nepoviruses showed that the *Aeonium* virus belongs to the subgroup A of the genus *Nepovirus* and is phylogenetically close to, but serologically distinct from tobacco ringspot virus (TRSV). Based on the species demarcation criteria for the family *Secoviridae*, the virus under study appears to be a novel member of the genus Nepovirus for which the name of *Aeonium* ringspot virus (AeRSV) is proposed.

Crassulaceae (Class *Magnoliopsida*, Order *Saxifragales*), a family of widely grown succulent ornamental plants comprises several genera, among which the genus *Aeonium*, a native of the Canary Islands that includes 37 species, most of which are herbaceous and perennial.

Recently, chlorotic spots and rings on both leaf surfaces were observed on several potted plants of an unidentified *Aeonium* species growing in private gardens of the city of Scafati (Campania, Italy) (Supplementary Fig. 1). An isometric virus was recovered by sap inoculation from symptomatic plants. On the basis of a preliminary sequence analysis of *ca.* 400 nucleotides (nt) of the 3′ untranslated (UTR) region of the viral genome (Sorrentino et al., 2012), it was identified as a strain or a variant of tobacco ringspot virus (TRSV), the type species of the genus *Nepovirus* (family *Secoviridae*, order *Picornavirales*; Sanfaçon et al., 2012). However, as the studies progressed, it became evident that the properties of the virus under study, hereafter referred to with the provisional name of Aeonium ringspot virus (AeRSV), differed enough from those of TRSV to warrant a more exhaustive characterization, which constitutes the object of this paper.

Sap from symptomatic *Aeonium* leaves was inoculated to a herbaceous host range comprising 19 species in six families. Inoculated plants were kept in a greenhouse at *ca.* 25 °C and observed up to four weeks for symptom expression. Most of the inoculated plants were infected showing overt symptoms (Table S1). In particular, *Nicotiana benthamiana* reacted with chlorotic/necrotic local lesions on inoculated leaves, frequently in the shape of ringspots, followed seven to ten days after inoculation by systemic symptoms consisting of extensive mottling and ringspots. A recovery phase took place about one week later, with production of symptomless leaves. Useful diagnostic hosts were *Chenopodium quinoa* and *C. murale* that reacted with local lesions followed by systemic infection, tip necrosis and death of the plant. The virus was routinely propagated in *N. benthamiana*, which was used for virus purification according to Pinck et al. (1988). Purified virus particles were resuspended in a small volume of 0.02 M sodium citrate buffer, pH 6.0. Concurrently, a TRSV isolate (obtained from Dr. M. Fuchs) was initially propagated in *N. benthamiana*. However, since at the greenhouse temperature (25–26 °C) these plants showed no symptoms, although systemically infected, *C. quinoa* plants were preferred for virus purification following the same protocol (Pinck et al., 1988).

AeRSV was readily purified from *N. benthamiana* plants with average yields of *ca.* 0.1 mg/g fresh tissue. Purification was also attempted from infected *Aeonium* plants, but the yield was much lower (*ca.* 0.01 mg/g tissue). Preparations negatively stained in

* Corresponding author. Tel.: +39 080 5442936; fax: +39 080 5442911.
** Corresponding author. Tel.: +39 081 2539365; fax: +39 081 2539367.
   E-mail addresses: alioto@unina.it (D. Alioto), l.rubino@ba.ivv.cnr.it (L. Rubino).
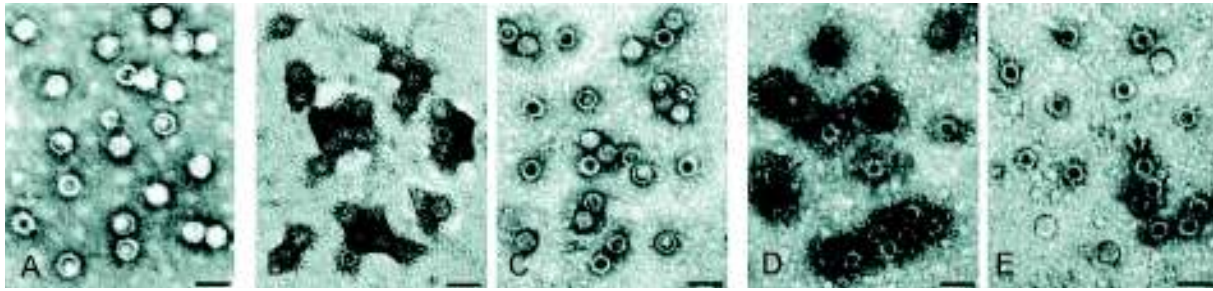
Fig. 1. (A) Negatively stained purified unfractionated AeRSV particles, fully, partially or not penetrated by the stain. (B and C) AeRSV particles exposed to the homologous or to TRSV antiserum, respectively. (D and E) TRSV particles exposed to the homologous or to AeRSV antiserum, respectively. Bars = 50 nm.

2% aqueous uranyl acetate and viewed at the electron microscope contained isometric particles *ca.* 30 nm in diameter, some of which partially or totally (empty shell) penetrated by the stain (Fig. 1A). An antiserum was produced by injecting purified virus preparations (0.5–2 mg) mixed with an equal volume of Freund's incomplete adjuvant in a New Zealand rabbit. Serological testing was done in agar gel double diffusion (Noordam, 1973) and immunoelectron microscopy (Milne and Lesemann, 1984). The antiserum to AeRSV had a titre of 1:256 as determined in agar gel double-diffusion tests. It gave a single clear-cut precipitin line with the homologous antigen in agar plates and no detectable reaction with TRSV and healthy plant extracts (not shown). In immunoelectron microscopy this antiserum decorated AeRSV particles from crude sap (not shown) or purified preparations (Fig. 1B), but not TRSV particles (Fig. 1E). Conversely, an antiserum against TRSV decorated purified TRSV (Fig. 1D), but not AeRSV (Fig. 1C) particles.

The cytopathological features of AeRSV were studied in systemically infected leaves of *N. benthamiana* processed according to standard procedures (Martelli and Russo, 1984). Compared with the healthy control (not shown), the structural organization of infected *N. benthamiana* cells was fairly well preserved, except for the presence of conspicuous inclusion bodies made up of accumulations of membranous vesicles with a fibrillar content, a network of proliferated endoplasmic reticulum strands, lipid droplets and virus particles (Fig. 2A). These cytopathological structures were usually appressed to the nuclei, the outer membrane of which was dilated in several points (Fig. 2B). Virus particles were either scattered in the ground cytoplasm or arranged in rows within tubular structures usually connected with plasmodesmata and sometimes associated with cell wall outgrowths (Fig. 2C). The observed cytopathological modifications are in complete agreement with those typically induced by nepovirus infections (Martelli and Russo, 1984; Ritzenthaler et al., 2002; Gokalp et al., 2003).

Purified virus preparations were dissociated in the presence of Laemmli's buffer (1970). The coat protein (CP) subunits migrated as a single band with an estimated mol. wt of 54 kDa (Fig. 3A) in discontinuos 12.5% acrylamide gels.

RNA was extracted from *ca.* 200 µg purified virus particles by adding 1 vol of extraction buffer (100 mM glycine–NaOH, pH 9.0, containing 100 mM NaCl, 10 mM EDTA, 2% sodium dodecyl sulfate and 1% sodium lauroyl sarcosine) and 2 vol of water-saturated phenol. The aqueous phase was further extracted with equal volumes of phenol and chloroform, then chloroform alone, and precipitated with 2.5 vol of ethanol in the presence of 0.3 M sodium acetate, pH 5.5. RNA was resuspended in sterile deionized water. Denatured RNA was either visualized by ethidium bromide staining or transferred to nylon membranes and hybridized with a DIG-labelled probe corresponding to the last 200 nucleotides of the viral RNAs. As shown in Fig. 3B, the encapsidated viral genome separated into two bands (RNA1 and RNA2).

Total nucleic acids (TNA) were extracted as detailed in Dalmay et al. (1993). Briefly, about 100 mg leaf tissue were macerated in a cold mortar in the presence of 600 µl extraction buffer and 600 µl phenol, processed as described above and resuspended in sterile deionized water. Northern blot analysis confirmed that RNA1 and RNA2 were the only virus-related RNA species present both in virus particles (Fig. 3B) and TNA extracts from infected *N. benthamiana* tissues (Fig. 3C, lane 1). However, Northern blot analysis of extracts from infected *Aeonium* plants revealed the presence of an additional RNA species smaller than RNA2 (Fig. 3C, lane 2).

Approximately 2 µg of RNA extracted from virus particles were denatured by heating at 65 °C and used for the construction of a cDNA library with a cDNA Synthesis Module (Roche, USA). The double stranded cDNA was ligated to a *Sma*I-linearized, dephosphorylated pUC18, and cloned into *Escherichia coli* strain XL1-Blue
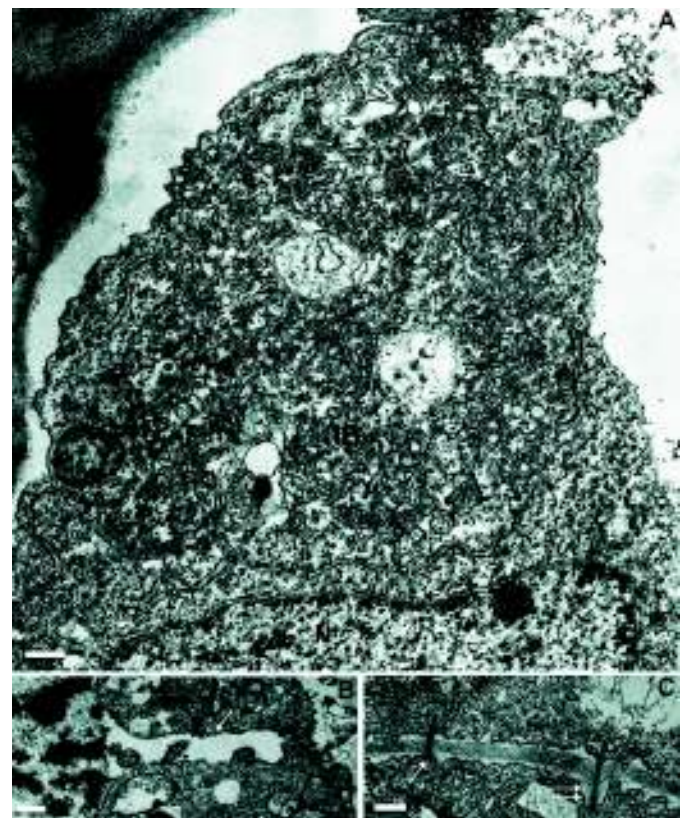

Fig. 2. Ultrastructural aspects of AeRSV-infected *N. benthamiana* mesophyll cells. (A) Vesiculate-vacuolate cytoplasmic inclusion bodies (IB) next to the nucleus (N). (B) Portion of a nucleus (N), showing enlargement of the outer membrane (arrow). (C) Virus-containing tubular structures connected with plasmodesmata (arrow) and inside developing cell wall outgrowth (double arrow). Bars = 250 nm.
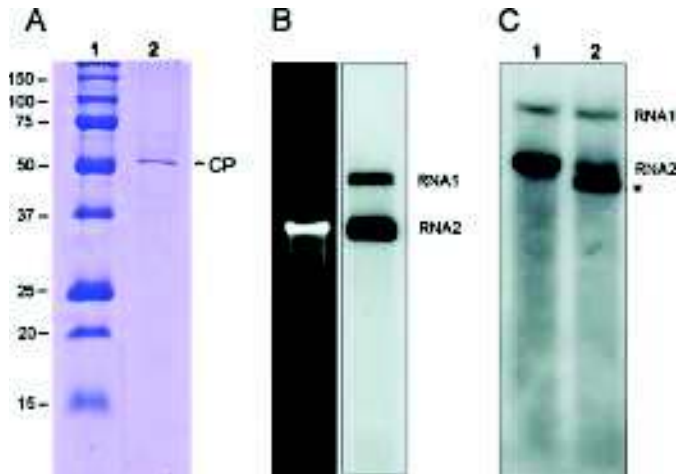
Fig. 3. Structural components of AeRSV. (A) SDS-polyacrylamide gel electrophoresis of dissociated virus particles. A single type of CP subunits *ca.* 54 kDa in size is visible (lane 2). Lane 1, molecular weight markers. (B) Genomic RNA1 and RNA2 from purified unfractionated particles visualized after ethidium bromide staining (left) or hybridization with a DIG-labelled probe (right). (C) Northern blot of RNA extracted from infected *N. benthamiana* (lane 1) and *Aeonium* (lane 2) leaves; hybridization as in panel B. The asterisk marks the additional RNA species found only in *Aeonium* extracts.

competent cells. The 5′ terminus of the viral genome was determined using a 5′ rapid amplification of cDNA ends (RACE) (Roche, USA). The 5′ RACE products were cloned into pGEM-T Easy vector (Promega, USA). Recombinant plasmids were purified with the NucleoSpin kit (Macherey-Nagel, Germany) and custom sequenced in both directions (Eurofins MWG Operon, Germany). Sequences thus obtained were bridged by RT-PCR using specific primers and high fidelity *Taq* DNA polymerase (Roche, USA). Sequences were assembled and analyzed using the DNA Strider software (Marck, 1988) and further examined by comparison with known nucleotide and protein sequences using BLAST (Altschul et al., 1990). Pairwise comparisons were made using EMBOSS in the EBI package (Rice et al., 2000). Sequences of the encoded proteins were aligned and tentative phylogenetic trees were constructed with ClustalW programme (Thompson et al., 1994) and visualized by the TreeView programme (Page, 1996).

RNA1 consists of 7549 nts, excluding the poly(A) tail (GenBank accession no. JX304792). The first AUG start codon is at nt position 104 in a context favourable to enhance translation in eukaryotic cells, with an A in position −3, a C in position −2 and a G in position +4 (Kozak, 2005). Assuming that translation begins at this AUG, it would terminate at the UAA stop codon at position 7046–7048, thus yielding a translation product (P1) of 2314 amino acids (aa) with a calculated M_r of 257,168 (257 kDa) (Fig. 4). Computer-assisted analysis showed that P1 contains the characteristic motifs of the putative viral protease cofactor (PRO-co), the NTP-binding (NTP-B),

Fig. 4. Putative schematic genome organization of AeRSV. Grey zones indicate conserved motifs in nepoviruses. Putative cleavage sites deduced by sequence comparison are indicated by the vertical lines. Dots in the 2A region indicate the position of two proline-rich sequences. Black circles indicate the putative VPg. RNA2′ represents the smaller RNA2 species, having a 179 aa deletion in the MP.

cysteine protease (PRO) and the RNA-dependent RNA polymerase (POL) core domains, indicating that the predicted polypeptide is cleaved by a viral protease to give mature functional products (Fig. 4). The putative viral protease cofactor motif (F-x_{21}-W-x_{11}-L-x_{22}-L-x-$\underline{T}$ between aa at positions 525–590) is slightly different from the consensus sequence for this motif (Rott et al., 1995), the major difference being the substitution of the last aa (E to T). The putative NTP-binding motif (Gorbalenya and Koonin, 1989) is located between aa 827 and 878, in two sites: site A between positions 827 and 834 (G-x_4-GKS) and site B (DD) at positions 877–878. The putative viral cysteine protease motif ($\underline{H}$-x_{35}-$\underline{E}$-x_{98}-$\underline{C}$G-x_8-G-x-x_5-G) is located between aa positions 1324 and 1475. The underlined aa H, E and C form the putative catalytic triad of the enzyme (Dessens and Lomonossoff, 1991; Gorbalenya et al., 1989; Margis and Pinck, 1992). The C-terminal region of P1 contains the sequence characterizing the putative RNA-dependent RNA polymerase (RdRp) (Argos, 1988) (D-x_4-D-x_{69}-G-x-x_3-T-x_3-N-x_{33}-GDD-x_{33}-DK) between aa postitions 1782 and 1936. The consensus sequence reported by Mayo and Fritsch (1994) for the genome-linked protein (VPg) was not found.

Amino acid alignments of AeRSV-encoded P1 with the comparable protein of selected nepoviruses allowed the prediction of putative cleavage sites and positions of mature products. For instance, comparison with the experimentally validated structure of the N-proximal region of arabis mosaic virus (ArMV) P1 (Wetzel et al., 2008), indicates that the N-terminal protease cofactor of the virus under study would be cleaved at the site C^{651}/G^{652} to separate from the NTB protein, and an additional cleavage site (C^{450}/S^{451}) would produce two protein domains of 450 and 201 aa, respectively, denoted X1 and X2. VPg is located between the NTP-binding and protease proteins, beginning at aa position 1254, as identified by comparison with the chemically determined N-terminal sequence of TRSV VPg (Zalloua et al., 1996). However, the rest of the sequence and the cleavage sites could not be established with certainty due to the low degree of conservation of this small protein. A cleavage site C^{1499}/S^{1500} separating the protease (*ca.* 215 aa) and RdRp (815 aa) proteins is predicted by comparison with the corresponding region of grapevine fanleaf virus (GFLV) P1 (Ritzenthaler et al., 1991; Margis et al., 1994).

RNA2 is 4010 nts in length, excluding the 3′-poly(A) tail (JQ670669). Its first AUG start codon at position 124–126 is preceded by a C in position −2 and followed by a G in position +4, *i.e.* in a less favourable translation context than that of RNA1. The single ORF of RNA2 extends from nt 124 to nt 3508–3510, yielding a putative polyprotein P2 of 1128 aa and a M_r of 125,601 (126 kDa) (Fig. 4). The polypeptide contains the "P" motif conserved in the movement proteins (MP) of nepoviruses and other plant viruses (Koonin et al., 1991; Mushegian, 1994) at aa position 442 and, at aa 1120–1123 the motif FWGR, that is very close to the nepovirus CP motif FYGR (Le Gall et al., 1995). The N-terminal peptide (approximately 260 aa) shares low sequence homology with protein 2A^{HP} of GFLV involved in the replication of RNA2 (Margis et al., 1993; Gaire et al., 1999; Ritzenthaler et al., 2002), including the proline motifs that are also present in tomato ringspot virus (ToRSV) P2 N-terminal protein (Carrier et al., 2001), suggesting this protein to have a role in the localization and replication of RNA2. Comparison of AeRSV CP sequence with the chemically determined sequence of TRSV CP (Buckley et al., 1993, 1995) indicated the A residue at position 616 as the N-terminal aa and a cleavage site M^{615}/A^{616} between the MP and CP proteins. Such M/A cleavage site between MP and CP is unusual and was reported only for another nepovirus (Tomitaka et al., 2011).

The smaller RNA species present only in infected *Aeonium* plants (Fig. 3C) was amplified by RT-PCR from purified viral RNA extracted from *Aeonium* using primers corresponding to the first and last 17 nts of both genomic RNAs. Molecular analysis showed that this
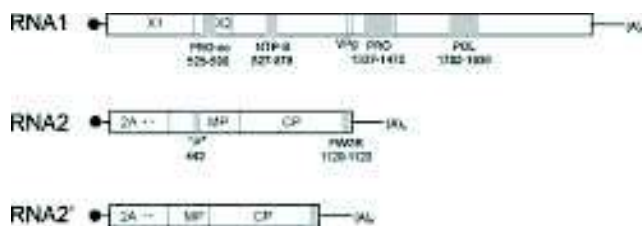
RNA is 3472 nts in length and has a sequence identical to that of RNA2 but lacks 537 nts from position 1286 to 1822. This additional RNA2 (RNA2′) has a single ORF that extends from the AUG at positions 124–126 and codes for a putative protein of 949 aa with a M_r of 105,726 (106 kDa) (Fig. 4). Putative maturation products of the polyprotein encoded by RNA2′ are the N-terminal protein (2A) and CP of the same size as those encoded by RNA2, and a MP with a deletion of 179 aa, from position 389 to position 567. At least two more examples of variability of nepoviral RNAs are known: one arising from RNA2 of ArMV (Loudes et al., 1995; Wetzel et al., 2002) and one from RNA1 of TBRV (Hasiów-Jaroszewska et al., 2012). However, only in the latter case some evidence of a possibile biological significance was obtained. The biological role of AeRSV RNA2′ has not yet been investigated.

Sequences of the 5′ UTR regions of the RNA1 (103 nts) and RNA2 (123 nts) were 53.2% identical. In particular, the first 17 nts (UUGAAAAUUCUCUCACA) are 100% identical and contain the 5′ end consensus sequence for nepovirus RNAs (underlined; Fuchs et al., 1989). The conserved repeats of the motif sequences capable to form stem-loop structures in the 5′ untranslated regions of other nepoviruses (Wetzel et al., 2001) were not found. Comparison between the 3′ UTR of RNA1 (501 nts) and RNA2 (500 nts) showed 98.6% identity.

Particle morphology, cytopathological features and genome organization support the classification of AeRSV in the genus *Nepovirus* (family *Secoviridae*, order *Picornavirales*; Sanfaçon et al., 2012), a taxon comprising three subgroups of species identified by differences in the cleavage sites recognized by their proteinase and size of RNA2: (i) subgroup A 3700–4000 nts; (ii) subgroup B 4440–4700 nts; (iii) subgroup C 6400–7300 nts. Based on these parameters, AeRSV fits well in subgroup A, a likelihood supported by its allocation next to TRSV in a clade of the phylogenetic tree constructed with CP sequences (Fig. S2).

Species demarcating criteria in the family *Secoviridae* set by the International Committe on Taxonomy of Viruses (ICTV) include, among others, lack of serological relationhip and less than 75%

identity in the aa sequence of CP and less than 80% in the aa sequence of the Pro-Pol region, defined as "the sequence contained between the protease CG and the polymerase GDD motifs" (Sanfaçon et al., 2012). When these and the whole P1 and P2 sequences were compared with those of nepoviruses of the three subgroups, the divergence between AeRSV and all the other viruses appeared to be well below the threshold for CP, whereas the Pro-Pol domain of TRSV was slightly above (84 *vs.* 80%) (Table 1). However, comparison of each single domain of TRSV and AeRSV polyproteins disclosed a relatively low percentage of identity throughout (Table S2).

The molecular data, the different reaction of infected *N. benthamiana* plants, and the lack of serological relationships support the notion that AeRSV is a novel nepovirus species phylogenetically close to but clearly distinct from TRSV.

Appendix A. Supplementary data

Supplementary data associated with this article can be found, in the online version, at http://dx.doi.org/10.1016/j.virusres.2013.08.012.

Table 1
Percentage of sequence identity between the amino acid sequences of various regions of AeRSV genome and those of other nepoviruses.

Virus	P1	P2	Pro-Pol	CP
Subgroup A				
ArMV	31	23	44	27
GDefV	30	20	42	25
GFLV	30	20	42	25
MMMoV	31	29	44	29
RpRSV	28	23	31	25
TRSV	78	70	84	66
Subgroup B				
BRSV	26	17	38	20
CNSV	28	19	36	20
GCMV	27	20	38	21
TBRV	27	20	40	25
Subgroup C				
BRV	27	17	38	23
CLRV	25	15	37	21
GBLV	27	16	42	21
ToRSV	27	15	38	23

GenBank accession numbers are: ArMV (arabis mosaic virus; NC_006057, NC_006056); GDefV (grapevine deformation virus; NC_017939, NC_017938); GFLV (grapevine fanleaf virus; NC_003615, NC_003623); MMMoV (melon mild mottle virus; AB518485, AB518486); RpRSV (raspberry ringspot virus; NC_005266, NC_005267); TRSV (tobacco ringspot virus; NC_005097, NC_005096); BRSV (beet ringspot virus; NC_003693, NC_003694); CNSV (cycas necrotic stunt virus; NC_003791, NC_003792); GCMV (grapevine chrome mosaic virus; NC_003622, NC_003621); TBRV (tomato black ring virus; NC_004439, NC_004440); BRV (blackcurrant reversion virus; NC_003509, NC_003502); CLRV (cherry leafroll virus; NC_015414, NC_015415); GBLV (grapevine Bulgarian latent virus; NC_015492, NC_015493); ToRSV (tomato ringspot virus; NC_003840, NC_003839).

References

Altschul, S.F., Gish, W., Miller, W., Myers, E.W., Lipman, D.J., 1990. Basic local alignment search tool. J. Mol. Biol. 215, 403–410.

Argos, P., 1988. A sequence motif in many polymerases. Nucleic Acids Res. 33, 145–156.

Buckley, B., Silva, S., Singh, S., 1993. Nucleotide sequence and in vitro expression of the capsid protein gene of tobacco ringspot virus. Virus Res. 30, 335–349.

Buckley, B., Silva, S., Singh, S., 1995. Corrigendum to "Nucleotide sequence and in vitro expression of the capsid protein gene of tobacco ringspot virus. Virus Res. 30, 335–349". Virus Res. 35, 111.

Carrier, K., Xiang, Y., Sanfaçon, H., 2001. Genomic organization of RNA2 of Tomato ringspt virus: processing at a third cleavage site in the N-terminal region of the polyprotein in vitro. J. Gen. Virol. 82, 1785–1790.

Dalmay, T., Rubino, L., Burgyan, J., Kollar, A., Russo, M., 1993. Functional analysis of cymbidium ringspot virus genome. Virology 164, 697–704.

Dessens, J.T., Lomonossoff, G.P., 1991. Mutational analysis of the putative catalytic triad of the cowpea mosaic virus 23 K protease. Virology 184, 738–746.

Fuchs, M., Pinck, M., Serghini, M.A., Ravelonandro, M., Walter, B., Pinck, L., 1989. The nucleotide sequence of satellite RNA in grapevine fanleaf virus, strain F13. J. Gen. Virol. 70, 955–962.

Gaire, F., Schmitt, C., Stussi-Garaud, C., Pinck, L., Ritzenthaler, C., 1999. Protein 2A of grapevine fanleaf nepovirus is implicated in RNA2 replication and colocalizes to the replication site. Virology 264, 25–36.

Gokalp, K., Digiaro, M., Cigsar, I., Abou Ghanem-Sabanadzovic, N., De Stradis, A., Boscia, D., Martelli, G.P., 2003. Properties of a previously undescribed nepovirus from South-East Anatolia. J. Plant Pathol. 85, 35–41.

Gorbalenya, A.E., Koonin, E.V., 1989. Viral proteins containing NTP-binding sequence pattern. Nucleic Acids Res. 17, 8413–8440.

Gorbalenya, A.E., Donchenko, A.P., Blinov, V.M., Koonin, E.V., 1989. Cysteine proteases of positive strand RNA viruses and chymotrypsin-like serine proteases. FEBS Lett. 243, 103–114.

Hasiów-Jaroszewska, B., Borodynko, N., Figlerowicz, M., Pospieszny, H., 2012. Two types of defective RNAs arising from the tomato black ring virus genome. Arch. Virol. 157, 569–572.

Koonin, E.V., Mushegian, A.R., Ryabov, E.V., Dolja, V.V., 1991. Diverse groups of plant RNA and DNA viruses share related movement proteins that may possess chaperone-like activity. J. Gen. Virol. 72, 2895–2903.

Kozak, M., 2005. Regulation of translation via mRNA structure in prokaryotes and eukaryotes. Gene 361, 13–37.

Laemmli, U.K., 1970. Cleavage of structural proteins during the assembly of the head of bacteriophage T4. Nature 227, 680–685.

Le Gall, O., Candresse, T., Dunez, J., 1995. A multiple alignment of the capsid protein sequences of nepoviruses and comoviruses suggests a common structure. Arch. Virol. 140, 2041–2053.

Loudes, A.M., Ritzenthaler, C., Pinck, M., Serghini, M.A., Pinck, L., 1995. The 119 kDa and 124 kDa polyproteins of arabis mosaic nepovirus (isolate S) are encoded by two distinct RNA2 species. J. Gen. Virol. 76, 899–906.

Marck, C., 1988. DNA Strider: a C programme for the fast analysis of DNA and protein sequences on the Apple Macintosh family computers. Nucleic Acids Res. 16, 1829–1836.

Margis, R., Pinck, L., 1992. Effects of site-directed mutagenesis on the presumed catalytic triad and substrate-binding pocket of grapevine fanleaf nepovirus 24-kDa proteinase. Virology 190, 884–888.

Margis, R., Ritzenthaler, C., Reinbolt, J., Pinck, M., Pinck, L., 1993. Genome organization of grapevine fanleaf nepovirus RNA2 deduced from the 122 K polyprotein P2 in vitro cleavage products. J. Gen. Virol. 74, 1919–1926.

Margis, R., Viry, M., Pinck, M., Bardonnet, N., Pinck, L., 1994. Differential proteolytic activities of precursor and mature forms of the 24 K proteinase of grapevine fanleaf nepovirus. Virology 200, 79–86.

Martelli, G.P., Russo, M., 1984. Use of thin sectioning for the visualization and identification of plant viruses. In: Maramorosch, K., Koprowski, H. (Eds.), Methods in Virology, vol. 8. Academic Press, New York, USA, pp. 143–224.

Mayo, M.A., Fritsch, C., 1994. A possible consensus sequence for VPg of viruses in the family Comoviridae. FEBS Lett. 354, 129–130.

Milne, R.G., Lesemann, D.E., 1984. Immunosorbent electron microscopy in plant virus studies. In: Maramorosch, K., Koprowski, H. (Eds.), Methods in Virology, vol. 8. Academic Press, New York, USA, pp. 85–101.

Mushegian, A.R., 1994. The putative movement domain encoded by nepovirus RNA-2 is conserved in all sequenced nepoviruses. Arch. Virol. 135, 437–441.

Noordam, D., 1973. Identification of Plant Viruses. Methods & Experiments. Centre for Agricultural Publishing and Documentation, Wageningen, The Netherlands.

Page, R.D., 1996. TreeView: an application to display phylogenetic trees on personal computers. Comput. Appl. Biosci. 12, 357–358.

Pinck, L., Fuchs, M., Pinck, M., Ravelonandro, M., Walter, B., 1988. A satellite RNA in grapevine fanleaf virus strain F13. J. Gen. Virol. 69, 233–239.

Rice, P., Longden, I., Bleasby, A., 2000. EMBOSS: the European Molecular Biology Open Software Suite. Trends Genet. 16, 276–277.

Ritzenthaler, C., Viry, M., Pinck, M., Margis, R., Fuchs, M., Pinck, L., 1991. Complete nucleotide sequence and genetic organization of grapevine fanleaf nepovirus RNA1. J. Gen. Virol. 72, 2357–2365.

Ritzenthaler, C., Laporte, C., Gaire, F., Dunoyer, P., Schmitt, C., Duval, S., Piéquet, A., Loudes, A.M., Rohfritsch, O., Stussi-Garaud, C., Pfeiffer, P., 2002. Grapevine fanleaf virus replication occurs on endoplasmic reticulum-derived membranes. J. Virol. 76, 8808–8819.

Rott, M.E., Gilchrist, A., Lee, L., Rochon, D.M., 1995. Nucleotide sequence of tomato ringspot virus RNA 1. J. Gen. Virol. 76, 465–473.

Sanfaçon, H., Gorbalenya, A.R., Knowles, N.J., Chen, J.P., 2012. Order Picornavirales. In: King, A.M.Q., Adams, M.J., Carstens, E.B., Lefkowitz, E.J. (Eds.), Virus Taxonomy. Classification and nomenclature of Viruses. Ninth Report of the International Committee on Taxonomy of Viruses. Elsevier Inc., pp. 835–839.

Sorrentino, R., Alioto, D., Russo, M., Rubino, L., 2012. Presence of tobacco ringspot virus in *Aeonium* spp. J. Plant Pathol. 94, S4.103.

Thompson, J.D., Higgins, D.G., Gibson, T.J., 1994. Clustal W: improving the sensitivity of progressive multiple sequence alignment through sequence weighting, position-specific gap penalties and weight matrix choice. Nucleic Acids Res. 22, 4673–4680.

Tomitaka, Y., Usugi, T., Yasuda, F., Okayama, H., Tsuda, S., 2011. A novel member of the genus *Nepovirus* isolated from *Cucumis melo* in Japan. Phytopathology 101, 316–322.

Wetzel, T., Meunier, L., Jaeger, U., Reustle, G.M., Krczal, G., 2001. Complete nucleotide sequences of the RNAs 2 of German isolates grapevine fanleaf and Arabis mosaic nepoviruses. Virus Res. 75, 139–145.

Wetzel, T., Fuchs, M., Bobko, M., Krzcal, G., 2002. Size and sequence variability of the Arabis mosaic virus protein 2A. Arch. Virol. 147, 1643–1653.

Wetzel, T., Chislom, J., Bassler, A., Sanfaçon, H., 2008. Characterization of proteinase cleavage sites in the N-terminal region of the RNA 1-encoded polyprotein from arabis mosaic virus (subgroup A nepovirus). Virology 375, 159–169.

Zalloua, P.A., Buzayan, J.M., Bruening, G., 1996. Chemical cleavage of 5′-linked protein from tobacco ringspot virus genomic RNAs and characterization of the protein-RNA linkage. Virology 219, 1–8.